

## SUPPORTING INFORMATION

### Quinoline based probe for effective and selective sensing of aspartic acid in aqueous medium: *In vitro* and *in vivo* live cell imaging

C. Elamathi,<sup>a</sup> R. J. Butcher,<sup>b</sup> A. Mohankumar,<sup>c</sup> P. Sundararaj,<sup>c</sup> A. Madankumar,<sup>d</sup>  
P. Kalaivani<sup>e</sup> and R. Prabhakaran<sup>\*a</sup>

<sup>a</sup>Department of Chemistry, Bharathiar University, Coimbatore- 641 046, India

<sup>b</sup>Department of Inorganic and Structural Chemistry, Howard University, Washington DC 20059

<sup>c</sup>Department of Zoology, Bharathiar University, Coimbatore 641 046, India

<sup>d</sup>Cancer Biology Lab, Molecular and Nanomedicine Research Unit, Sathyabama Institute of Science and Technology, Chennai 600 119, India

<sup>e</sup>Department of Chemistry, Nirmala College for women, Bharathiar University, Coimbatore - 641046.

## 1. Experimental Section

### Materials and methods

8-methyl-2-oxo-1,2-dihydroquinoline-3-carbaldehyde was synthesized according to the literature procedure.<sup>1</sup> All other organic chemicals and inorganic salts were available from commercial sources and used without further purification. Infrared spectra were taken on a Jasco FT-IR 400-4000 cm<sup>-1</sup> range using KBr pellets. Electronic spectra were recorded on a JASCO 600 spectrophotometer and fluorescence property was measured using a JASCO FP-6600 spectrofluorometer at room temperature (298 K). <sup>1</sup>H NMR, spectra were recorded in DMSO at room temperature with a Bruker 400 MHz instrument, chemical shift relative to tetramethylsilane. The chemical shifts are expressed in parts per million (ppm). HRMS mass spectra were recorded on Bruker mass spectrometer. Single crystal data collections and corrections for **8MPS** and **8MPSC** were done at 293 K with CCD Kappa Diffractometer using graphite mono chromated Mo Ka ( $k = 0.71073$  Å) radiation.<sup>2</sup> The structural solution were done by using SHELXS-97 and refined by full matrix least square on *F*<sup>2</sup> using SHELXL-2014.<sup>3</sup>

### Synthesis of **8MPS** (8-methyl-2-oxo-1,2-dihydroquinoline-3-carboxaldehyde-4(*N*)-phenylsemicarbazone)

8-Methyl-2-oxo-1,2-dihydroquinoline-3-carboxaldehyde (1 g, 5 mmol) in 25 cm<sup>3</sup> of methanol was taken in a Schlenk flask and was degassed with continuous flow of nitrogen. To this methanolic solution of 4-phenylsemicarbazide (0.997 g, 5 mmol) was added by dropwise. Finally, the mixture was degassed again with nitrogen and was refluxed with constant stirring. A yellow precipitate was formed immediately and was further refluxed with

stirring about 30 minutes. The formed product was filtered and recrystallized with DMF/MeOH mixture which afforded suitable crystals for X-ray diffraction studies. Yield: 89 %, Mp: 289 °C. FT-IR (KBr disks,  $\text{cm}^{-1}$ ): 1658( $\nu_{\text{C=O}}$ ) (oxo); 1600( $\nu_{\text{C=N}}$ ) and 1658( $\nu_{\text{C=O}}$ ) (ketoamide). UV-vis (ethanol:water (1:5),  $\lambda_{\text{max}}(\text{dm}^3 \text{ mol}^{-1} \text{ cm}^{-1})$ : 287 (49,788) nm ( $\pi \rightarrow \pi^*$  transition); 326 (72,777) nm and 363 (79,964) nm ( $n \rightarrow \pi^*$  transition);  $^1\text{H}$  NMR (DMSO- $d_6$ , ppm):  $\delta$  11.82 (s, 1H, N(3)H),  $\delta$  10.82 (s, 1H, N(1)H),  $\delta$  8.84 (s, 1H, N(4)H),  $\delta$  8.60 (s, 1H, -CH=N),  $\delta$  8.11 (s, 1H, C(4)H),  $\delta$  7.53 (s, 1H, C(5)H),  $\delta$  7.595-7.597 (d, 1H, C(6)H),  $\delta$  7.574-7.576 (d, 1H, C(7)H),  $\delta$  7.355-7.380 (d, 1H, C(2)H for terminal phenyl),  $\delta$  7.239-7.260 (d, 1H, C(6)H for terminal phenyl),  $\delta$  7.303-7.343 (t, 1H, C(3)H for terminal phenyl),  $\delta$  7.007-7.064 (t, 1H, C(4)H for terminal phenyl),  $\delta$  2.27 (s, 3H, -CH<sub>3</sub>, C(8) position).

### Preparation of stock solutions for cationic colorimetric titrations

Stock solution of **8MPS** was prepared (20 mM in ethanol: water (1:5)) at pH = 7.2. The solutions of the guest cations ( $\text{Al}^{3+}$ ,  $\text{Ca}^{2+}$ ,  $\text{Co}^{3+}$ ,  $\text{Cr}^{3+}$ ,  $\text{Fe}^{3+}$ ,  $\text{Fe}^{2+}$ ,  $\text{Cu}^{2+}$ ,  $\text{Mn}^{2+}$ ,  $\text{Ni}^{2+}$ ,  $\text{Zn}^{2+}$ ,  $\text{Hg}^{2+}$  and  $\text{Co}^{2+}$ ) using their chloride salts in the concentration of 10  $\mu\text{M}$  were prepared in aqueous solution. Solutions of various concentrations containing host and increasing concentrations of cations were prepared separately. The spectra of these solutions were recorded by means of absorbance as well as fluorescence methods. Where  $\text{Cu}^{2+}$  was added gradually to **8MPS** and fluorescence spectra were recorded. For fluorescence study, excitation wavelength used was 391 nm (excitation slit = 5.0 nm and emission slit = 5.0 nm). A series of solutions containing **8MPS** (20  $\mu\text{M}$  in ethanol: water (1:5)) and copper ion (chloride) (20  $\mu\text{M}$ ) in aqueous solution were prepared in such a manner, the sum of the volume of total metal ion and **8MPSC** remained constant (4 mL) at pH 7.2. Job's plots were drawn by plotting  $\Delta F$  versus mole fraction of  $\text{Cu}^{2+}$  (chloride).<sup>4</sup>

A similar procedure was adopted by preparing the stock solutions for fluorescent probe, and different L-amino acids such as arginine (Arg), alanine (Ala), valine (Val), asparagine (Aspara), leucine (Leu), aspartic acid (Asp), glutamic acid (Glu), histidine (His), phenylalanine (Phenylala), proline (Pro) and threonine (Thr) in 10  $\mu\text{M}$  concentration, which were added to the solutions of **8MPSC**. The spectra of these solutions were recorded both absorbance and fluorescence methods. Where aspartic acid was added gradually to both the solutions of **8MPSC**, emission intensity increases gradually. For fluorescence study, excitation wavelength used was 390 nm (excitation slit = 5.0 and emission slit = 5.0). A series of solutions containing **8MPSC** (20  $\mu\text{M}$ ) and aspartic acid (20  $\mu\text{M}$ ) were prepared in such a manner that the sum of the total volume of **8MPSC** and aspartic acid remained constant (4 mL) (**8MPSC** = **8MPS** in ethanol: water (1:5), and  $\text{Cu}^{2+}$  in (chloride) in aqueous

solution, at pH 7.2. Job's plots were drawn by plotting  $\Delta F$  versus mole fraction of aspartic acid.<sup>5</sup>

### **MCF-7 live cell bio-imaging**

MCF-7 cells were seeded on cover slips in six well plates for overnight with RPMI media and 10% FBS. On the next day cells were treated with **A- 8MPS (20 mM)**, **B- (8MPS (20 mM) + Cu<sup>2+</sup>(chloride) (10  $\mu$ M))** and **C-(8MPS (20 mM) + Cu<sup>2+</sup> (chloride) (10  $\mu$ M)) + Aspartic acid (10  $\mu$ M))** respectively for 1 h, at a dose of 10  $\mu$ M. After treatment, cells were fixed with methanol and washed with 0.5% Phosphate buffer saline Tween (PBST) twice and then with 1 $\times$ PBS thrice. The cover slips were mounted on slides using glycerol. The slides were observed under fluorescent microscope (Leica DM4000 B, Germany) under 20X magnification.<sup>6</sup>

### ***C. elegans* maintenance and culture conditions**

Wild-type N2 *C. elegans* was obtained from the Caenorhabditis Genetics Centre (University of Minnesota, MN, USA) and maintained on to the nematode growth media agar plates spotted with *E. coli* OP50 (uracil auxotrophs) at 20°C as described previously.<sup>7,8</sup> For age synchronization, eggs were extracted using sodium hydroxide-sodium hypochlorite solution from gravid adult worms and then maintained in M9 medium (6 g Na<sub>2</sub>HPO<sub>4</sub>, 3 g KH<sub>2</sub>PO<sub>4</sub>, 5 g NaCl, 0.25 g MgSO<sub>4</sub>.7H<sub>2</sub>O and 1 L deionized water) at 20°C to favour the hatching.<sup>9</sup>

### **Feeding, imaging and image analysis**

The age-synchronized L4 larvae of wild-type N2 worms (n=35-40/experiment) were exposed to PBS buffer solution containing 20 mM of **8MPS** for 6 h at 20°C. After exposure, the worms were washed thrice with PBS buffer. The worms were then exposed to 10  $\mu$ M **Cu<sup>2+</sup>(chloride)** for 4 h at room temperature. For aspartic acid treated samples, previously exposed L4 stage worms were transferred to eppendorf tube filled with 1 mL of PBS buffer and 10  $\mu$ M of aspartic acid at 20°C for 4 h. At the end of treatment, the worms were collected and washed three time with PBS buffer before being mounted on a 3 % agar padded microscopic slides. The imaging of immobilized live worms were taken using upright fluorescence microscope (BX41, Olympus, Japan) which was equipped with a digital camera (E330, Olympus, Japan). The captured images were analyzed for fluorescence signal by determining the mean pixel intensity using image J software and the acquired data was subjected to one-way analysis of variance (ANOVA) followed by bonferroni post-hoc test (SPSS 17, IBM Corporation, NY, USA).<sup>9</sup>

## **X-ray crystallography study**

### **Hydrogen bonding for 8MPS**

An intermolecular hydrogen bonding gave a pseudo bimolecular structure to the compound (Fig. S2, 3† and Table S2†). In addition, first unit of hydrogen atom of quinoline nitrogen N(1) bonded to oxygen atom of solvent moiety, which is present in the lattice unit N(1)-H(1A)···O(3)#1. Bond formation between hydrogen atom of imine nitrogen N(3) of second unit and oxygen atom O(1) of oxo group which is exist in first unit N(3)-H(3B)···O(1)#1.

### **Hydrogen bonding for 8MPSC**

Four different types of intermolecular hydrogen bonding were found in **8MPSC**, as shown in (Table S2†). First type is hydrogen atom of coordinated water molecule bonded to coordinated chloride ion Cl(1)#1 in first unit. Similar type of hydrogen bonding was observed in second type, in this case hydrogen atom of coordinated water molecule bonded to chloride ion Cl(2)#2 in lattice unit, which was present in second unit. Third type was hydrogen atom of quinoline nitrogen N(1) bonded to chloride ion Cl(2)#3 in asymmetric unit, which is also present in third unit. Last type of bond is formed between hydrogen atom of imine nitrogen N(3) bonded to chloride ion in lattice unit Cl(2). The above four hydrogen types bonding are making a zig zag type of complex. Molecular packing and hydrogen bonding diagrams are shown in (Fig. S11,12†).

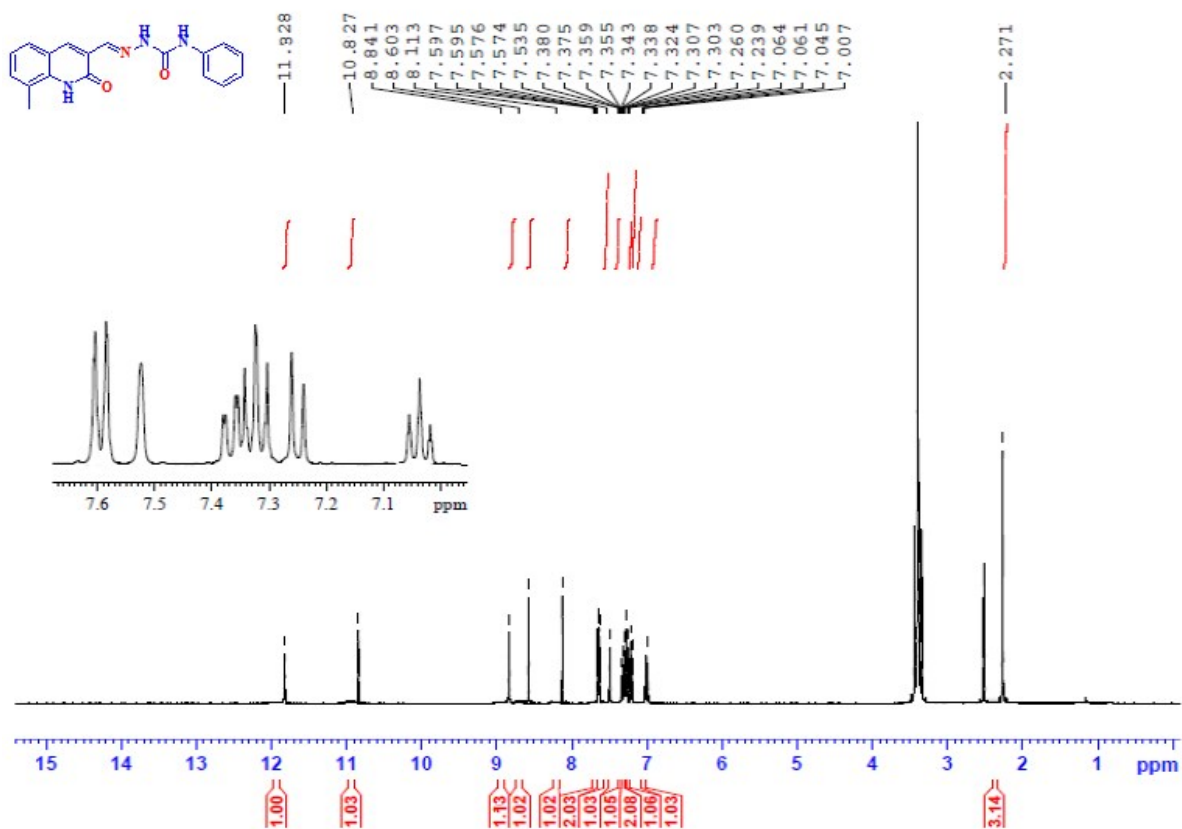


Fig. S1. <sup>1</sup>H NMR spectrum (DMSO-d<sub>6</sub>) of **8MPS**.

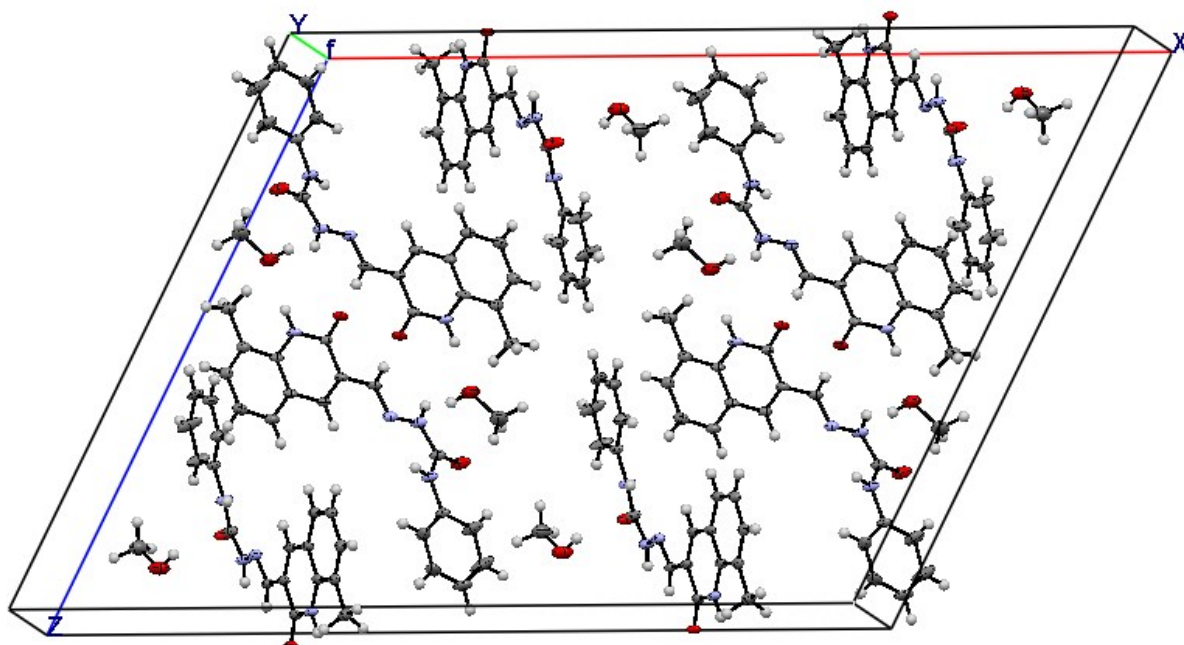


Fig. S2. Molecular packing diagram for **8MPS**.

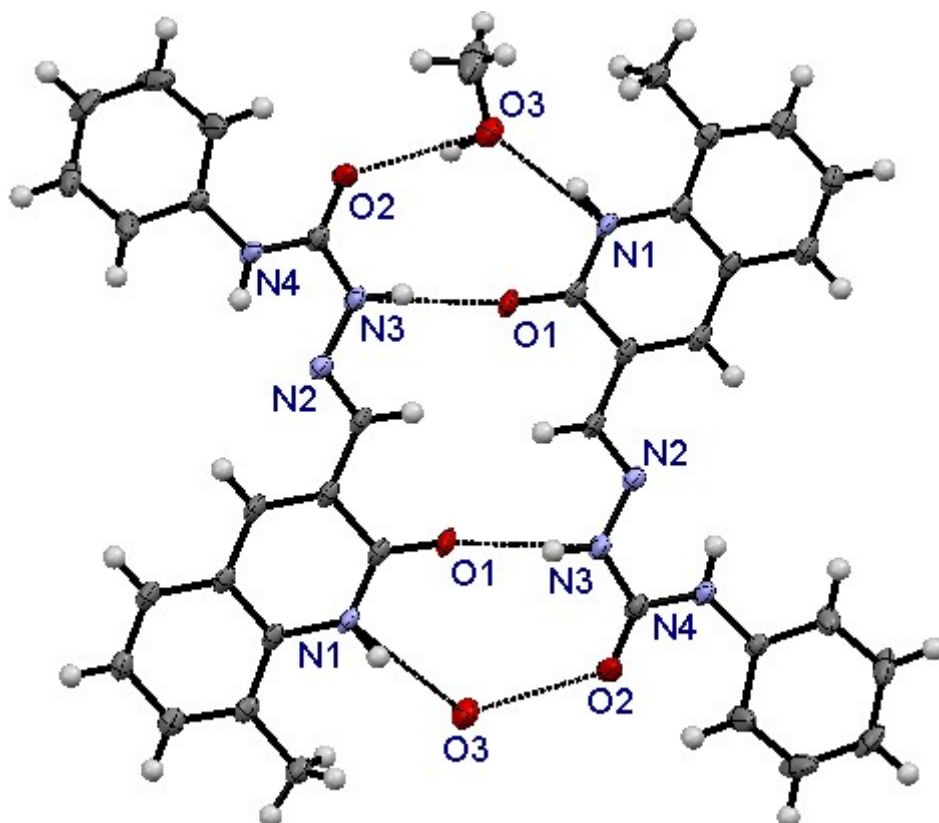


Fig. S3. Hydrogen bonding diagram for **8MPS**.

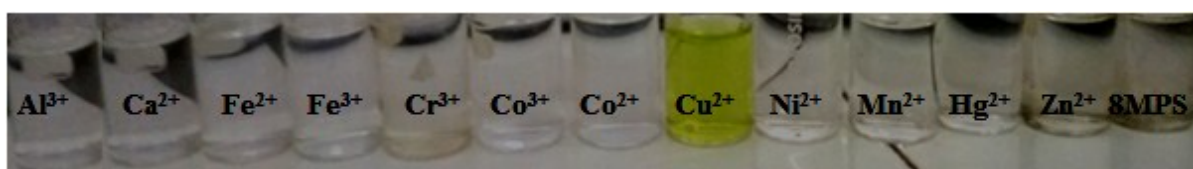


Fig. S4. Changes in colour under visual inspection of **8MPS** with chloride salts of different cations.



Fig. S5. Naked eye visual inspection of **8MPS** (20 mM in ethanol: water (1:5)) towards different copper salts (10  $\mu$ M) in aqueous solution. 1- Copper sulphate, 2- Copper acetate and 3- Copper nitrate.

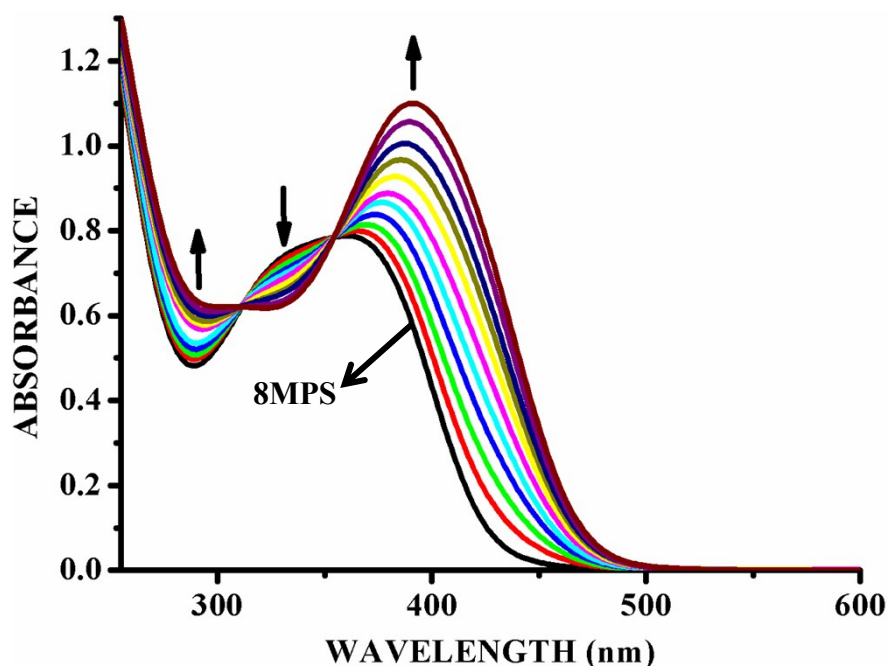


Fig. S6. Changes in the UV-vis spectrum of **8MPS** (20 mM; ethanol: H<sub>2</sub>O (1:1 v/v)) upon gradual addition of Cu<sup>2+</sup>(chloride; 10 μM) in aqueous solution at pH = 7.2.

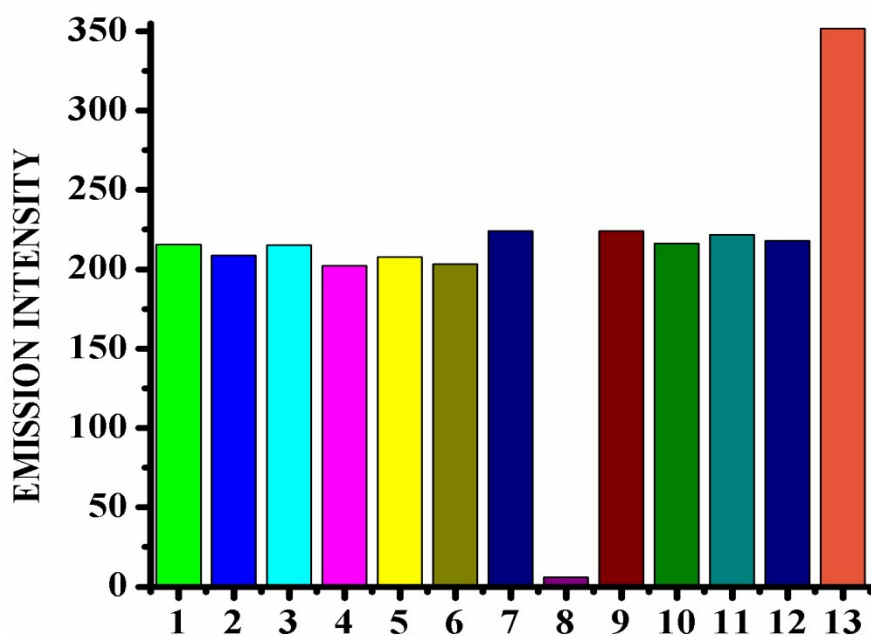


Fig. S7. Fluorescence emission spectra of **8MPS** (20 mM, ethanol: H<sub>2</sub>O (1:5)) in the presence of chloride salts of different cations (10 μM), 1- Al<sup>3+</sup>, 2- Ca<sup>2+</sup>, 3- Co<sup>3+</sup>, 4- Cr<sup>3+</sup>, 5- Fe<sup>3+</sup>, 6- Fe<sup>2+</sup>, 7- Mn<sup>2+</sup>, 8- Cu<sup>2+</sup>, 9- Ni<sup>2+</sup>, 10- Zn<sup>2+</sup>, 11- Hg<sup>2+</sup>, 12- Co<sup>2+</sup> in aqueous solution and 13- blank (**8MPS**).

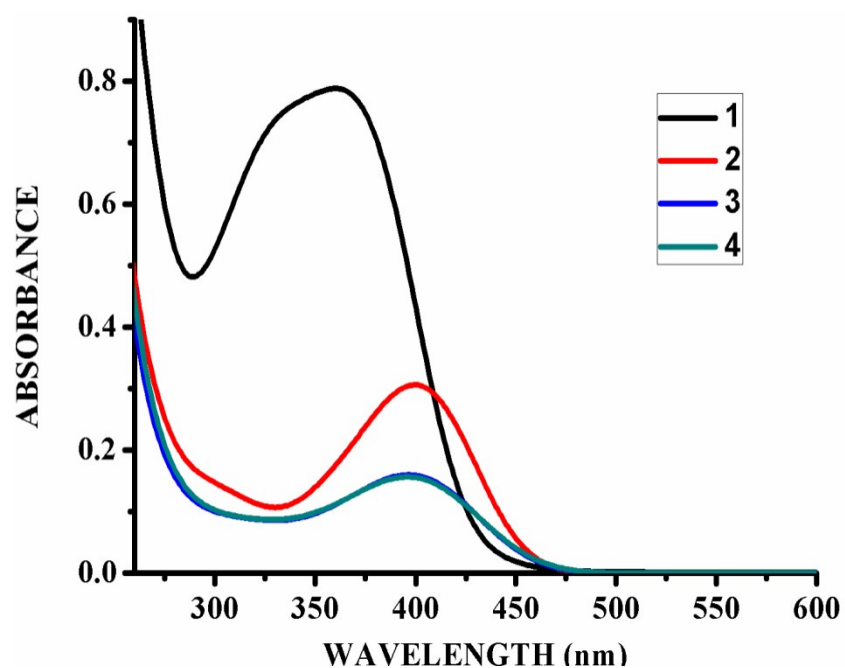


Fig. S8. Absorption spectra of **8MPS** (20 mM in ethanol: water (1:5)) with various copper salts (10 μM). 1-8MPS, 2-Copper nitrate, 3- Copper acetate and 4- Copper sulphate.

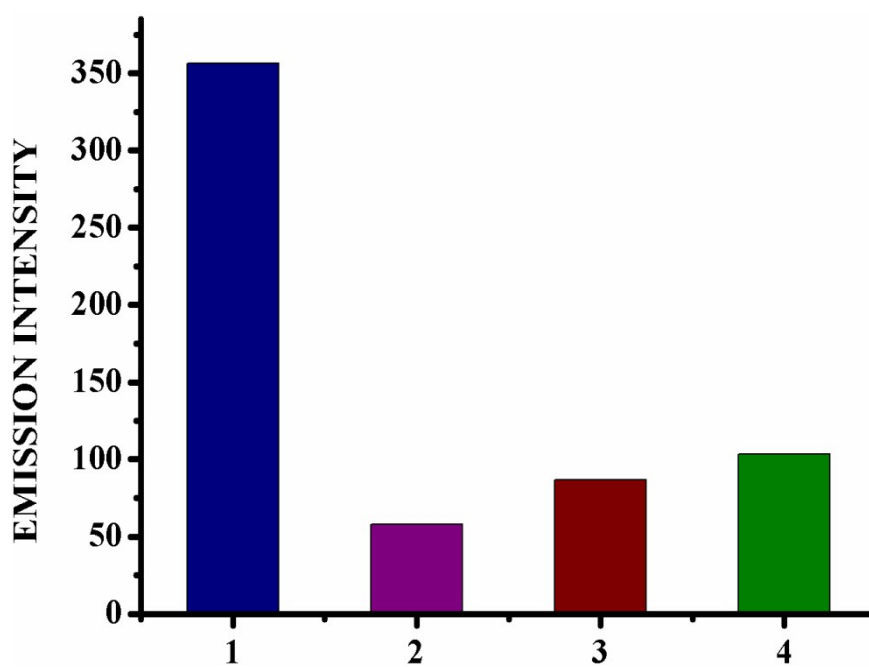


Fig. S9. Fluorescence spectra of **8MPS** (20 mM in ethanol: water (1:5)) with various copper salts (10 μM). 1-8MPS, 2-Copper nitrate, 3- Copper acetate and 4- Copper sulphate.



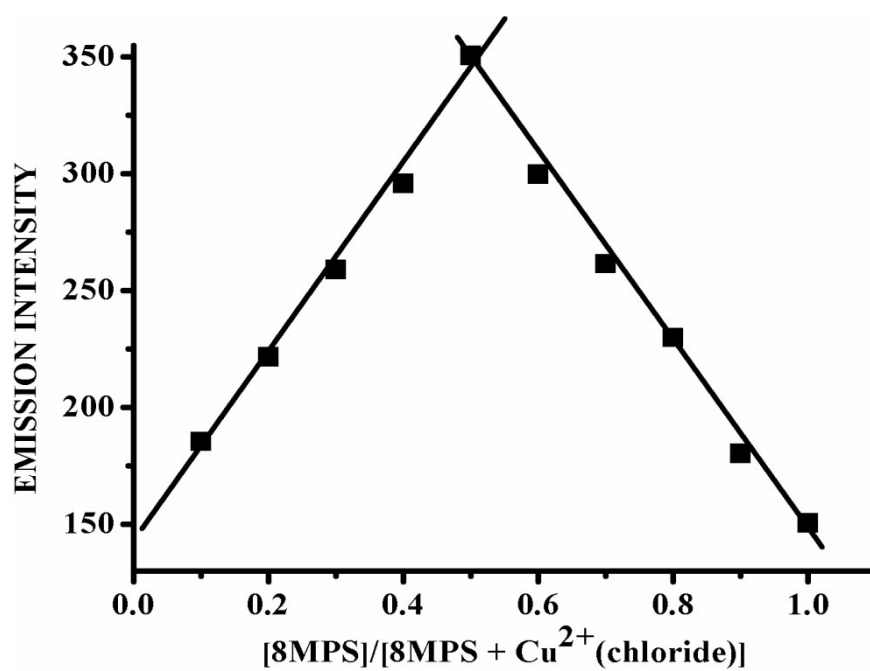


Fig. S10. Job's plot of **8MPS** and Cu<sup>2+</sup> ([**8MPS**] + [Cu<sup>2+</sup> (chloride)]) = 40 μM.

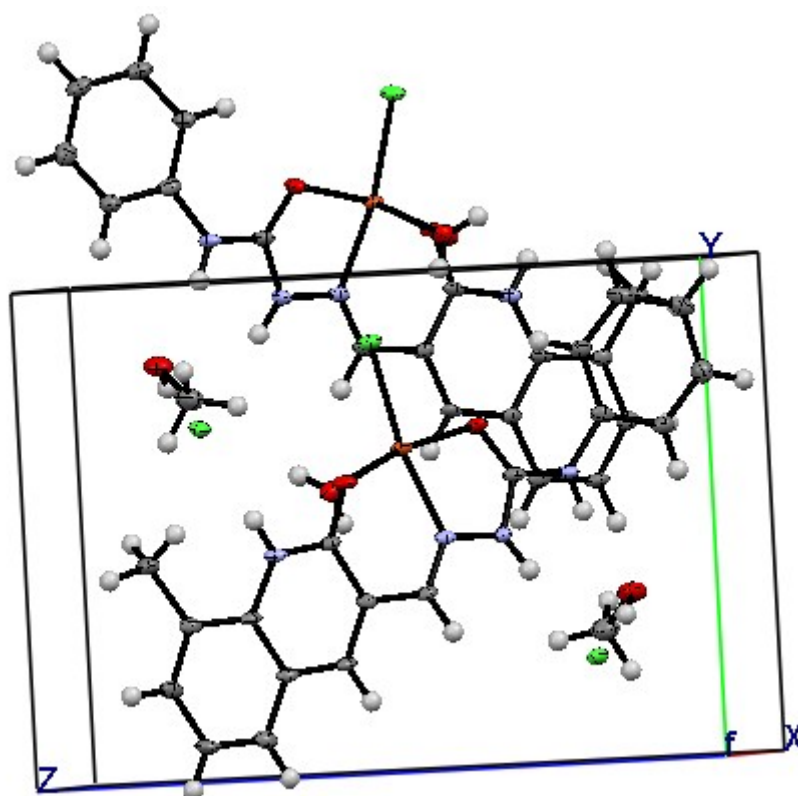


Fig. S11. Molecular packing diagram for **8MPSC**.

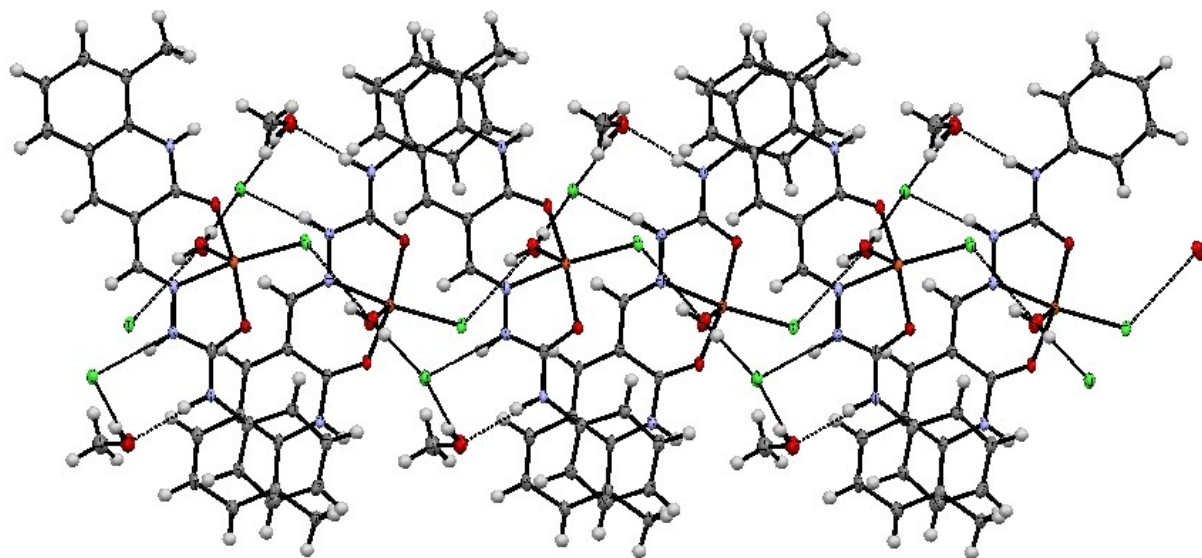


Fig. S12. Hydrogen bonding diagram for **8MPSC**.

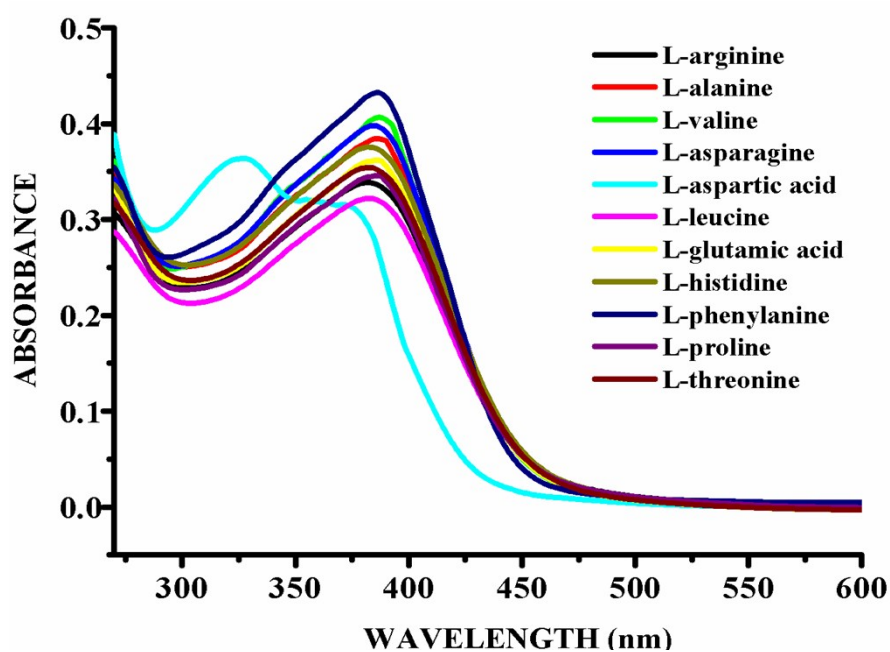


Fig. S13. Absorption spectra of **8MPSC** (the complex of 20 mM **8MPSC** in ethanol: water (1: 5) and 10  $\mu\text{M}$   $\text{Cu}^{2+}$ ) in presence of various amino acids (all amino acids in 10  $\mu\text{M}$ ) in aqueous solution. 1- ala; 2- arginine; 3- valine; 4- asparagine; 5- aspartic acid; 6- leucine; 7- glutamic acid; 8- histidine; 9- phenylalanine; 10- proline; 11- threonine.

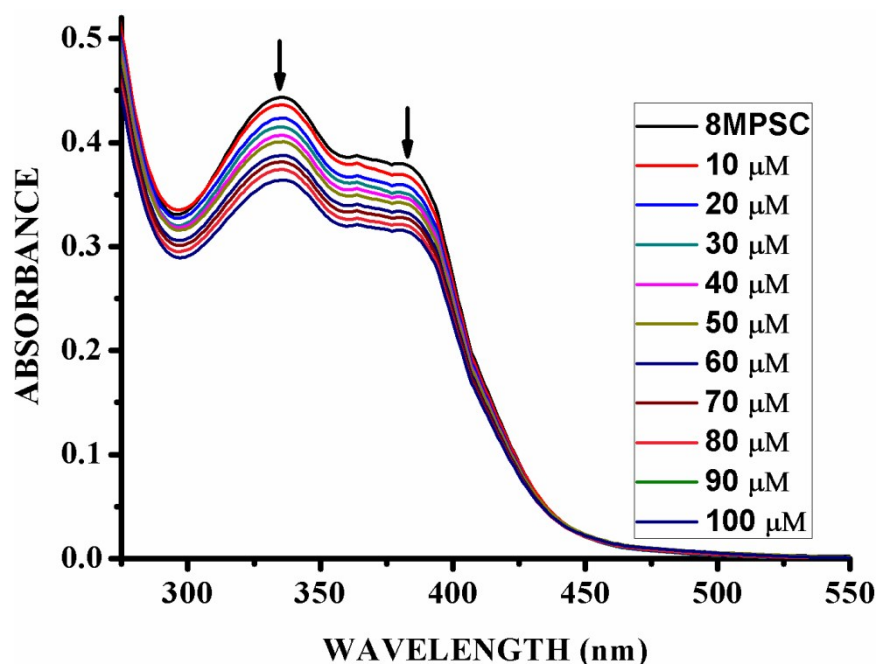


Fig. S14. Absorption titration spectra of **8MPSC** (10  $\mu\text{M}$ ) upon gradual addition of aqueous solution of in 10  $\mu\text{M}$  concentration.

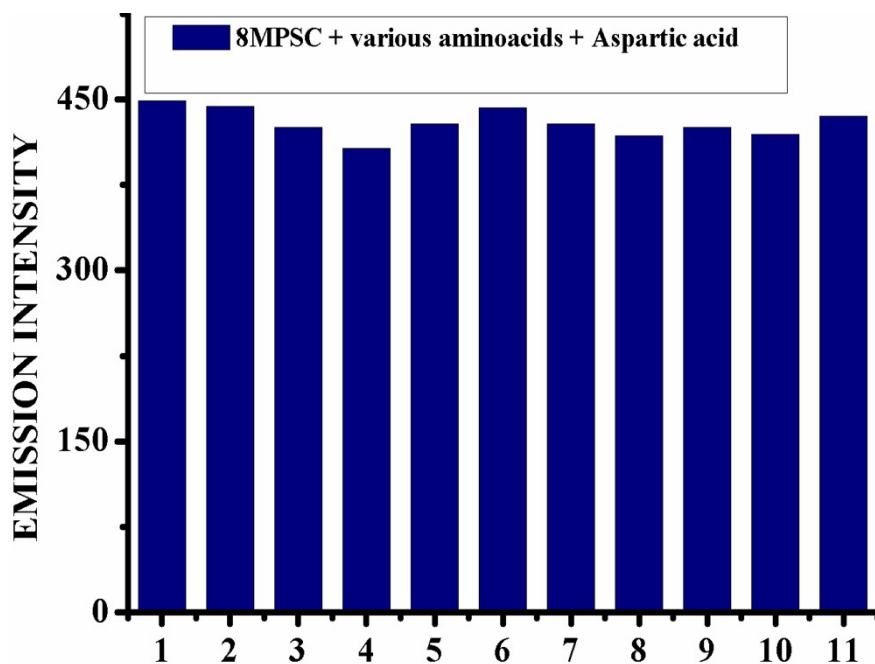


Fig. S15. Fluorescence spectra of **8MPSC** (the complex of 20 mM **8MPS** and 10  $\mu\text{M}$   $\text{Cu}^{2+}$ ), various amino acids (10  $\mu\text{M}$ ) and Aspartic acid (Asp) (10  $\mu\text{M}$ ). 1- **8MPSC** + alanine + Asp; 2- **8MPSC** + arginine + Asp; 3- **8MPSC** + valine + Asp; 4- **8MPSC** + asparagine + Asp; 5- **8MPSC** + leucine + Asp; 6- **8MPSC** + glutamic acid + Asp; 7- **8MPSC** + histidine + Asp; 8- **8MPSC** + phenylalanine + Asp; 9- **8MPSC** + proline + Asp; 10- **8MPSC** + threonine + Asp and 11- **8MPSC** + Asp.

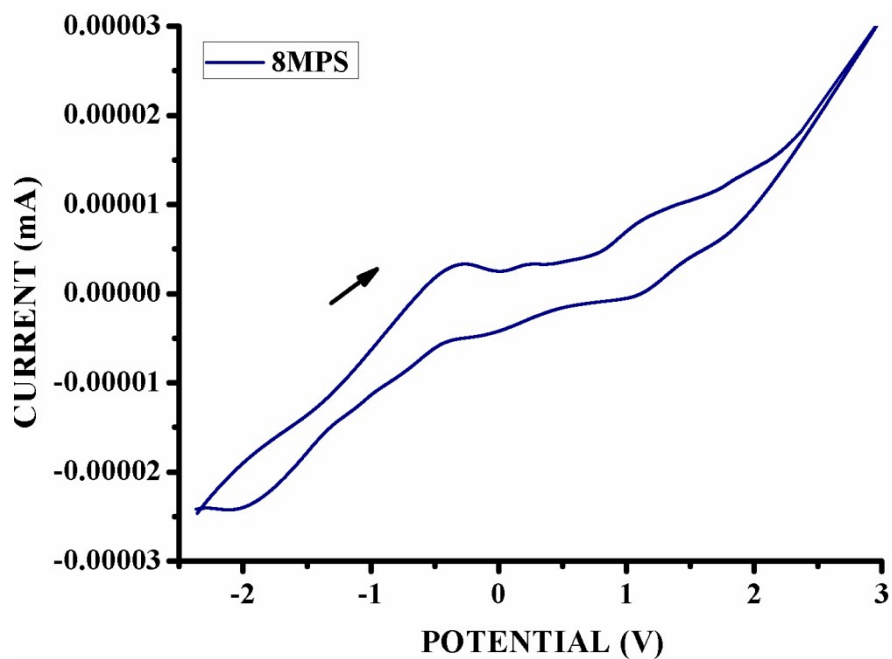


Fig. S16. Cyclic voltammogram study for 10  $\mu\text{M}$  concentration of **8MPS** in DMF solvent using platinum wire counter electrode, platinum disc working electrode and non-aqueous Ag/AgCl reference electrode and tetrabutylammonium perchlorate as a supporting electrolyte.

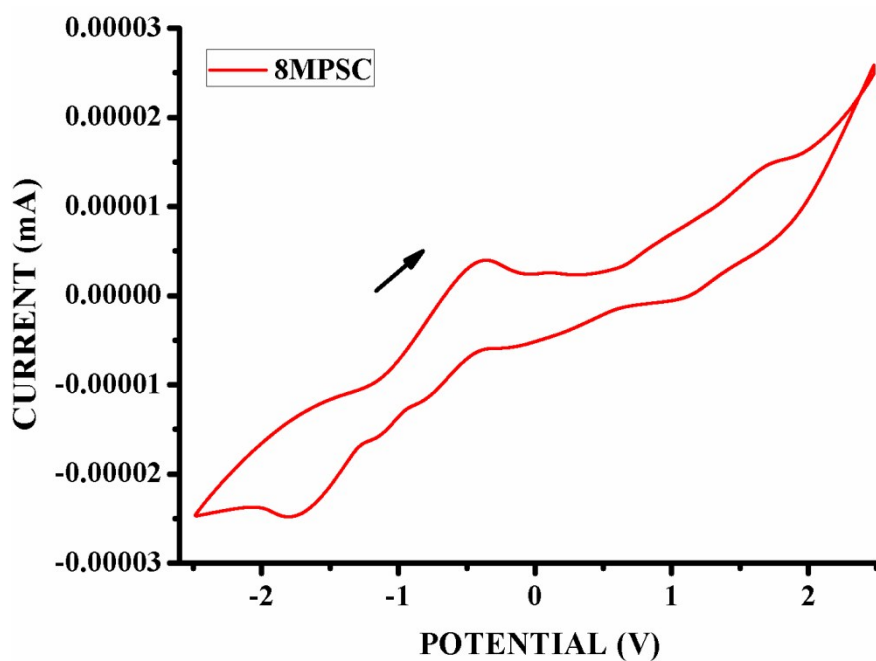


Fig. S17. Cyclic voltammogram study for 10  $\mu\text{M}$  concentration of **8MPSC** in DMF solvent using platinum wire counter electrode, platinum disc working electrode and non-aqueous Ag/AgCl reference electrode and tetrabutylammonium perchlorate as a supporting electrolyte.

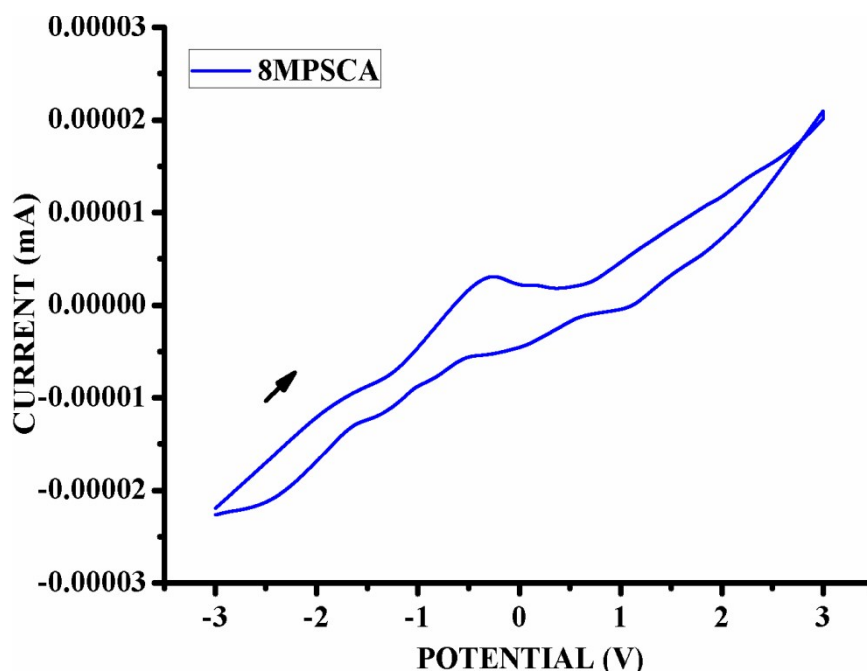


Fig. S18. Cyclic voltammogram study for 10  $\mu$ M concentration of **8MPSCA** in DMF solvent using platinum wire counter electrode, platinum disc working electrode and non-aqueous Ag/AgCl reference electrode and tetrabutylammonium perchlorate as a supporting electrolyte.

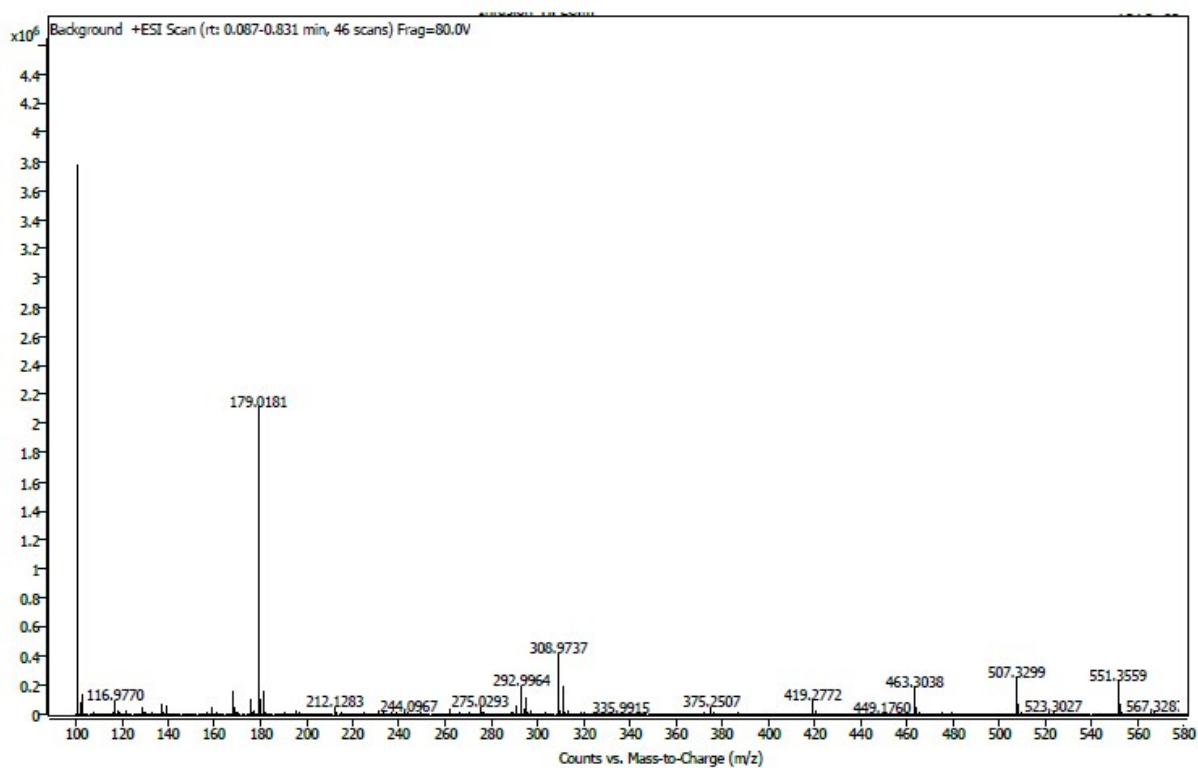


Fig. S19. Mass spectrum of **8MPSCA**.

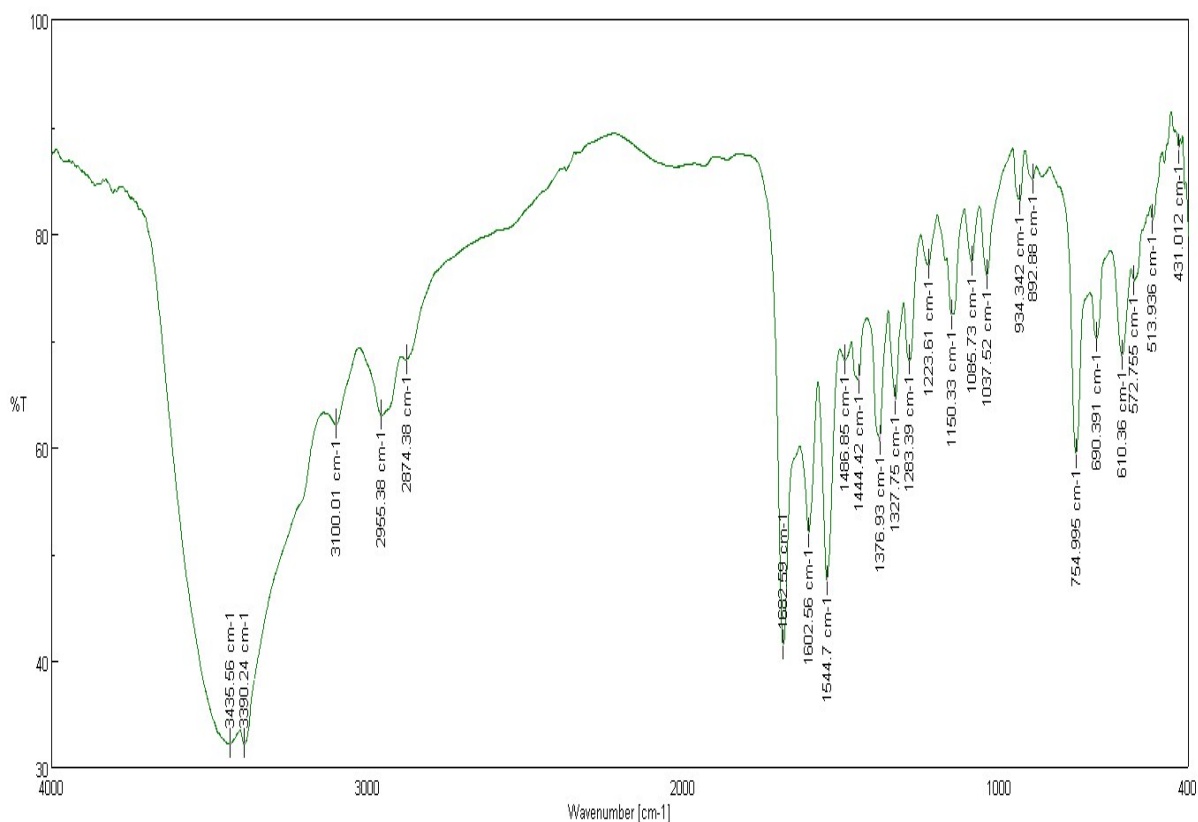


Fig. S20. FT-IR spectrum of **8MPS**.

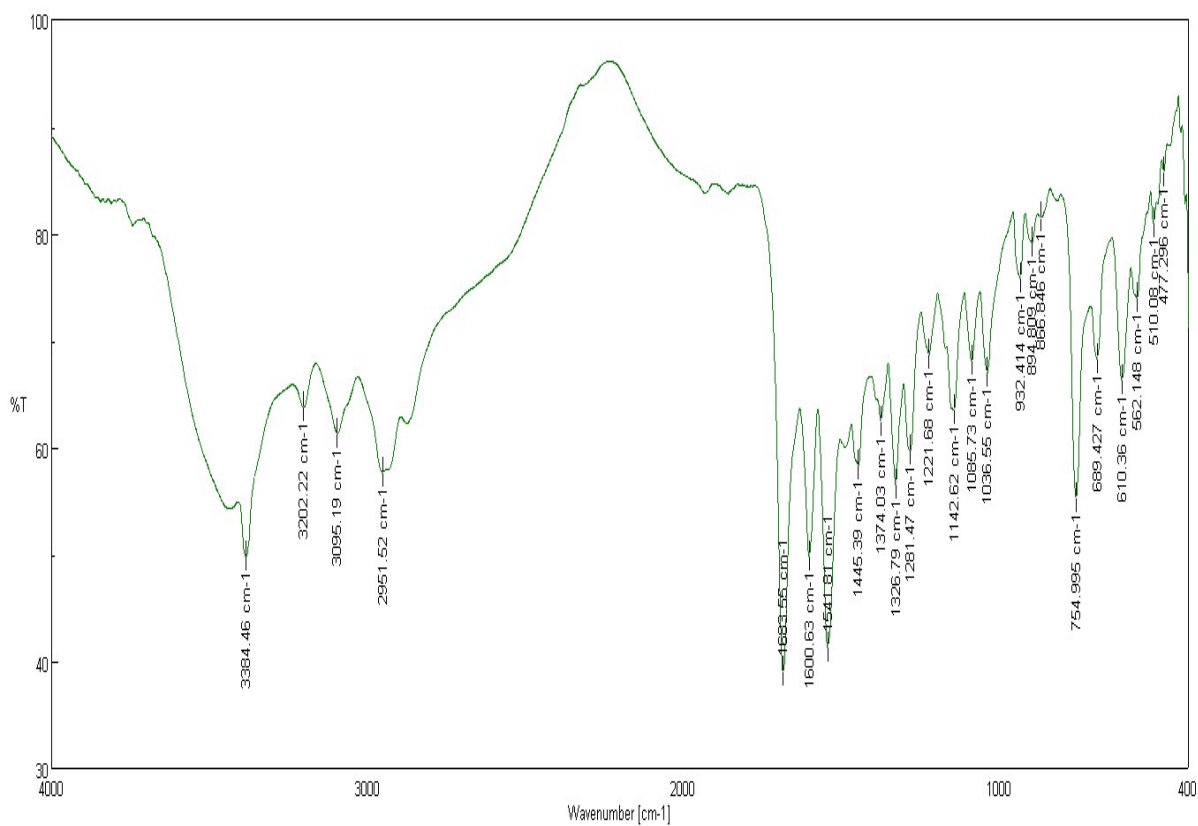


Fig. S21. FT-IR spectrum of **8MPSC**.

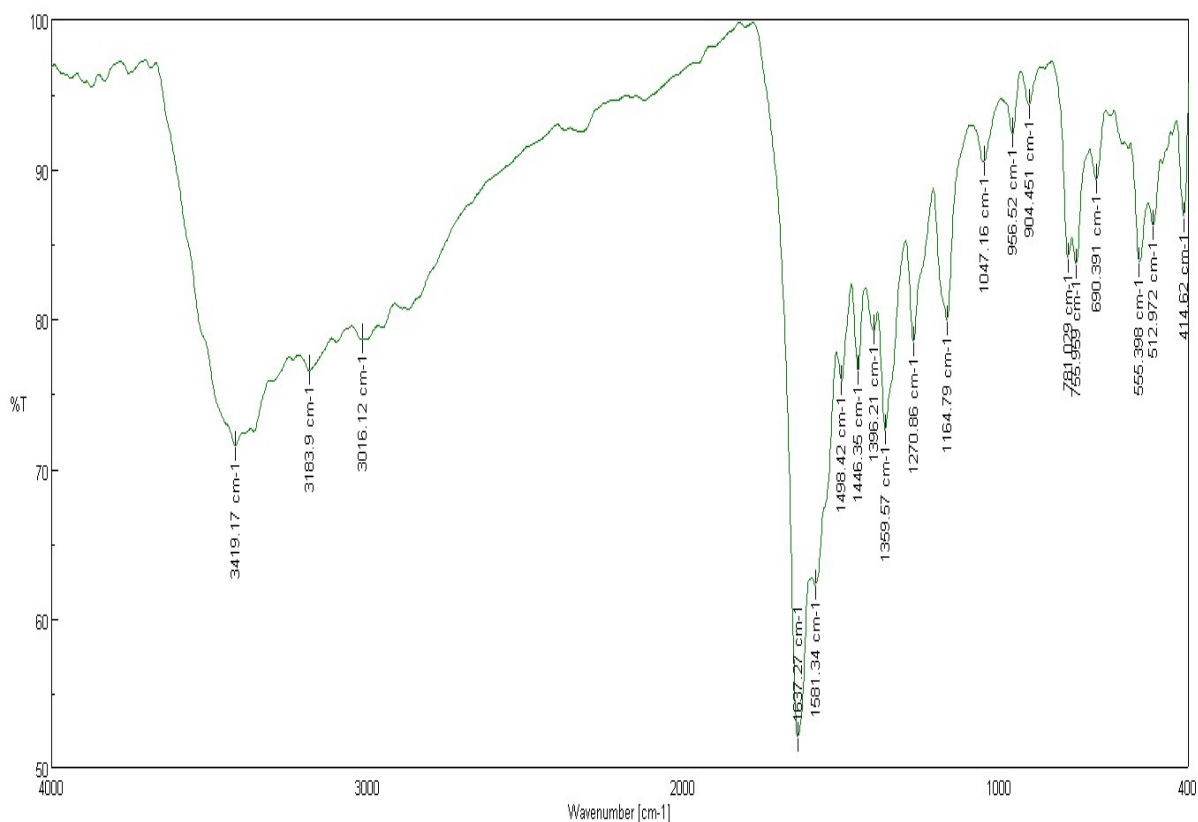


Fig. S22. FT-IR spectrum of **8MPSCA**.

Table S1 Bond lengths Å and bond angles [°] for **8MPSC**

Bond Lengths		Bond Angles	
Cu-O(1)	1.947(3)	O(1)-Cu-N(2)	89.61(15)
Cu-N(2)	1.978(4)	O(1)-Cu-O(2)	165.73(14)
Cu-O(2)	1.982(3)	N(2)-Cu-O(2)	80.66(15)
Cu-Cl(1)	2.2346(12)	O(1)-Cu-Cl(1)	93.80(10)
Cu-O(1W)	2.299(4)	N(2)-Cu-Cl(1)	169.28(12)
		O(2)-Cu-Cl(1)	94.02(9)
		O(1)-Cu-O(1W)	93.28(15)
		N(2)-Cu-O(1W)	84.04(15)
		O(2)-Cu-O(1W)	96.04(15)
		Cl(1)-Cu-O(1W)	105.87(10)

Table S2 Hydrogen bond distances for **8MPS** and **8MPSC**

<b>D-H...A</b>	<b>d(D-H)</b>	<b>d(H...A)</b>	<b>d(D...A)</b>	<b>&lt;(DHA)</b>
<b>8MPS</b>				
O(3)-H(3)···O(2)	0.84	1.96	2.737(3)	154.3
N(1)-H(1A)···O(3)#1	0.88	2.08	2.929(3)	161.0
N(3)-H(3B)···O(1)#1	0.88	1.97	2.838(3)	169.2
N(4)-H(4N)···O(2)#2	0.88	2.50	3.203(3)	137.0
Symmetry transformations used to generate equivalent atoms: #1 -x+3/2,-y+3/2,-z+1 #2 x,y-1,z				
<b>8MPSC</b>				
O(1W)-H(1W1)···Cl(1)#1	0.82(3)	2.49(4)	3.428(4)	154(6)
O(1W)-H(1W2)···Cl(2)#2	0.81(3)	2.35(3)	3.160(4)	175(6)
N(1)-H(1A)···Cl(2)#3	0.88	2.58	3.343(4)	145.2
N(3)-H(3B)···Cl(2)	0.88	2.30	3.130(4)	157.2
Symmetry transformations used to generate equivalent atoms: #1 -x+1,y-1/2,-z+1 #2 -x+1,y+1/2,-z+1 #3 -x+2,y+1/2,-z+1				

Table S3 Elemental analyses and FT-IR spectroscopy of **8MPS**, **8MPSC** and **8MPSCA**

<b>Comp ounds</b>	<b>Elemental analyses</b>			<b>IR spectral data in cm<sup>-1</sup></b>					
	<b>Calculated (Found) %</b>								
	<b>C</b>	<b>H</b>	<b>N</b>	<b><math>\nu_{OH}</math></b>	<b><math>\nu_{C=O}</math> (ox o)</b>	<b><math>\nu_{C=N}</math></b>	<b><math>\nu_{C=O}</math> (keto amide)</b>	<b><math>\nu_{C=O}</math> (asym)</b>	<b><math>\nu_{C=O}</math> (sym)</b>
<b>8MPS</b>	67.49 (61.38)	5.03 (4.78)	17.49 (17.18)	-	1682	1544	1682	-	-
<b>8MPSC</b>	46.62 (44.78)	4.96 (3.67)	11.49 (10.12)	-	1683	1541	1683	-	-
<b>8MPSCA</b>	48.77 (45.87)	4.45 (3.78)	12.36 (10.14)	3419	1637	1581	1637	1637	1359



## References

1. F. E. Mabbs D. J. Machin, *Magnetism, Transition Metal Complexes*; Chapman and Hall: London, 1973.
2. R. H. Blessing, An empirical correction for absorption anisotropy, *Acta Crystallogr. Sect.*, 1995, **A51**, 33-38.
3. G. M. Sheldrick, SHELXTL Version 5.1, *An Integrated System for Solving, Refining and Displaying Crystal Structures from Diffraction Data*, Siemens Analytical X-ray Instruments, Madison, WI, 1990.
4. X. Lia, F. Huo, Y. Yue, Y. Zhang and C. A. Yina, *Sens. Actuators B*, 2017, **253**, 42–49.
5. H. Un, S. Wu, C. Huang, Z. Xuc and L. Xu, *Chem. Commun.*, 2015, **51**, 3143-3146.
6. S. Brenner, The genetics of *Caenorhabditis elegans*. *Genetics*, 1974, **77**, 71-94.
7. A. Mohankumar, G. Shanmugam, D. Kalaiselvi, C. Levenson, S. Nivitha, G. Thiruppathi and P. Sundararaj, *Rsc Adv.*, 2018, **8**, 33753-33774.
8. T. J. Fabian and T. E. Johnson, *J. Gerontol.*, 1994, **49**, B145–B156.
9. G. Devagi, A. Mohankumar, G. Shanmugam, S. Nivitha, F. Dallemer, P. Kalaivani, P. Sundararaj and R. Prabhakaran, *Sci. Rep.*, 2018, **8**, 7688. DOI:10.1038/s41598-018-25984-7.